JTTEE5 8:258-262

Peer Reviewed

Surface Protection of Light Metals by One-Step Laser Cladding with Oxide Ceramics

S. Nowotny, A. Richter, and K. Tangermann

(Submitted 5 June 1998; in revised form 12 January 1999)

Today, intricate problems of surface treatment can be solved through precision cladding using advanced laser technology. Metallic and carbide coatings have been produced with high-power lasers for years, and current investigations show that laser cladding is also a promising technique for the production of dense and precisely localized ceramic layers. In the present work, powders based on Al_2O_3 and ZrO_2 were used to clad aluminum and titanium light alloys. The compact layers are up to 1 mm thick and show a nonporous cast structure as well as a homogeneous network of vertical cracks. The high adhesive strength is due to several chemical and mechanical bonding mechanisms and can exceed that of plasma-sprayed coatings. Compared to thermal spray techniques, the material deposition is strictly focused onto small functional areas of the workpiece. Thus, being a precision technique, laser cladding is not recommended for large-area coatings. Examples of applications are turbine components and filigree parts of pump casings.

Keywords ceramic coating, cladding, laser, light metals, wear protection

1. Introduction

New lightweight material applications in the automotive and aircraft industries require advanced materials and techniques for surface protection of the related components. For this purpose, oxide ceramics are of special interest because of their low specific weight, low thermal conductivity, high chemical stability (especially at high temperatures), and good tribological properties. Plasma spraying is widely used in industry for the production of ceramic protection layers on light metals. This technique has been intensively developed during the last decades and in many cases provides the only means to meet the requirements for the surface properties.

However, the applications of thermal spraying are limited by the typical layer porosity, the restricted adhesive strength, and the inability to localize the coatings precisely (Ref 1-3). During subsequent laser densification of plasma-sprayed ceramic layers, it is difficult to avoid the creation of stress-dependent, uncontrollable cracks (Ref 4-7). In addition, this multistep process is not favorable with respect to fabrication and cost. The goal of the present work, therefore, was to develop the technique of one-step laser cladding with dynamic powder feed as a possible extension of the present spray technologies. Particular attention has been paid to the production of compact and dense layers with a higher adhesive strength and a more precise localization of the coating.

Currently laser deposition welding (cladding) is being used successfully to coat steel and other metallic materials with metal alloys, which can be reinforced with coarse-grained carbide particles (Ref 8). The fields of application are wear protection, remanufacturing, and precision treatment. In the relatively few publications dealing with the application of this method for the production of ceramic layers, steel was named for the most part as the substrate material (Ref 9-11), although a few references were made to the use of other alloys (Ref 12). Because of the increased use of aluminum and titanium alloys, especially in the transportation industry, the investigations of the underlying research project were performed using these substrate materials.

S. Nowotny, A. Richter, and **K. Tangermann,** Fraunhofer Institute for Material and Beam Technology, Winterbergstrasse 28, D-01277 Dresden, Germany. Contact e-mail: nowotny@iws.fhg.de.

2. Laser Technique

The principle of laser cladding is shown in Fig. 1. The process is carried out by blowing the ceramic powder into the laser-generated melt pool on the surface. While passing the laser

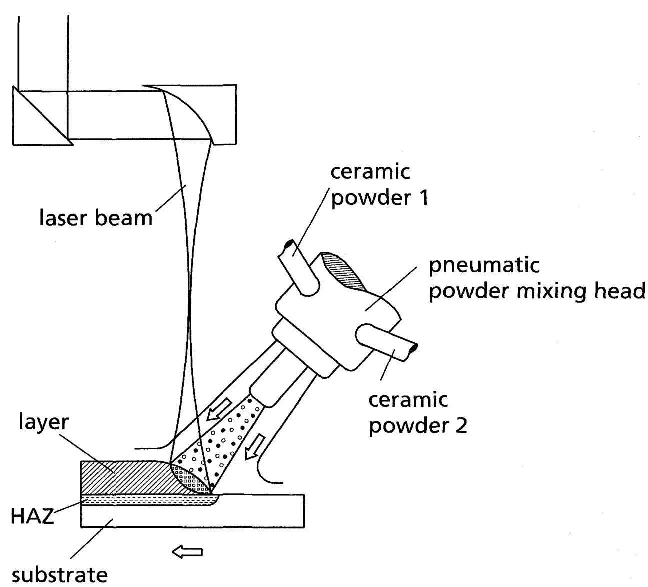

Fig. 1 Principle of one-step laser cladding with dynamic powder supply

beam, the powder is heated, but it only melts completely in the melt pool. In addition, well-controlled substrate fusing is an important precondition for obtaining a high adhesive strength. Heating and melting of the substrate proceed mainly by thermal conduction from the ceramic melt. The degree of substrate melting can be controlled by the laser energy input, the interaction time of the laser beam with the material, and the lifetime of the melt.

Cooling and solidification of the ceramic-metal compound proceed by heat conduction into the cool substrate volume. The cooling rates are not as high as during plasma spraying.

Single tracks with a width of 1.5 to 3 mm are produced. Wider surface zones are clad by overlapping these tracks.

For the present investigations, a 6 kW CO_2 continuous-wave laser was used as the beam source. The characteristic wavelength of 10.6 μm leads to an absorption coefficient of more than 90% for the ceramic melt. In this way, the laser energy is efficiently used for melting the ceramic powder completely, and the requirement of limited fusion of the base material can be fulfilled more easily. The process parameters were varied over a wide range in order to respond to the behavior of the different materials, to produce layers of different shapes, and to determine the effects of the different parameters. As a result, the following limits of the main process parameters were found: laser beam power of 500 to 2000 W, cladding speed of 150 to 600 mm/min, powder feed rate of 4 to 12 g/min, and track overlap degree of 15 to 50%.

For the powder supply, a double-hopper powder feeder, based on a plasma spray device and optimized for laser cladding, was used. Two powder components, independently fed by this feeder system, were pneumatically mixed in a cyclone mixing head and led through a nozzle into the melt pool.

3. Materials

As substrate materials, the alloys AlSi10Mg and TiAl6V4 were chosen because of their increasing importance in the automotive and aircraft industries. The ceramic powders used are listed in Table 1. Al_2O_3 was selected as the main ceramic component due to its high wear resistance, low price, and chemical similarity to the aluminum substrates. Mullite and TiO_2 additions, as well as a mixture of Al_2O_3 and ZrO_2-Y_2O_3, were used due to their improved flow and wetting and toughness properties. In addition, ZrO_2-Y_2O_3, widely used for the production of thermal barrier coatings, were included in the investigations.

The following discussion focuses on the Al_2O_3/TiO_2 system deposited onto AlSi10Mg because of its highly advanced state of development. Comparisons to other material systems will be made.

Table 1 Composition and grain size of the powders

Material	Composition, wt%	Grain size, μm
Al_2O_3	…	45-90
Al_2O_3/TiO_2	87/13	45-75
Al_2O_3/Mullite(a)	75/25	38-90
ZrO_2/Y_2O_3	93/7	45-90
Al_2O_3/ZrO_2-Y_2O_3	84/16	45-90

(a) Mullite = 70% Al_2O_3 + 30% SiO_2

4. Characterization of the Ceramic Coatings

4.1 Structure

Al_2O_3-Based and ZrO_2-Based Ceramics on AlSi10Mg. The layers produced by laser cladding (Fig. 2) have a smooth surface and a parameter-dependent thickness of 0.1 to 1.0 mm. The Al_2O_3/TiO_2 (87/13) coatings exhibit a dense, pore-free cast structure and regularly formed vertical cracks, making them suitable for thermomechanical loading (Fig. 3).

X-ray diffraction and scanning electron microscopy (SEM) with energy dispersive x-ray analysis (EDXA) were used to analyze the ceramic coatings. From the x-ray pattern, the main component of the coatings was found to be α-Al_2O_3 (corundum), the

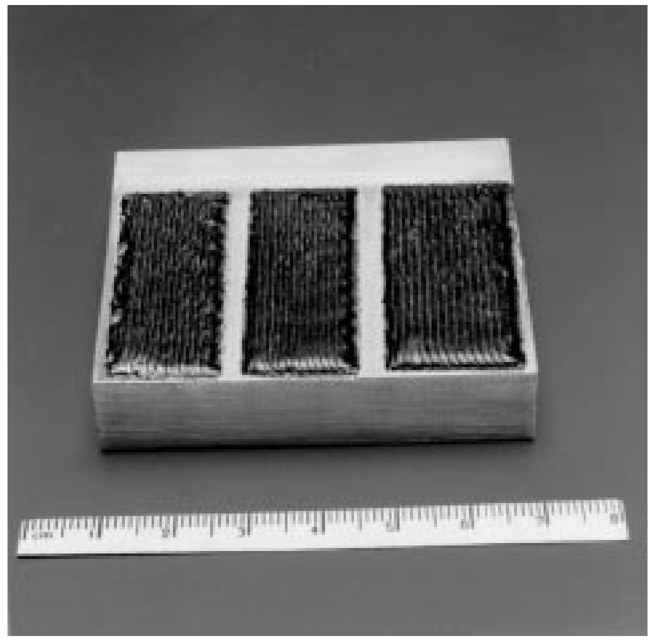

Fig. 2 Al_2O_3/TiO_2 layers on an AlSi10Mg sample

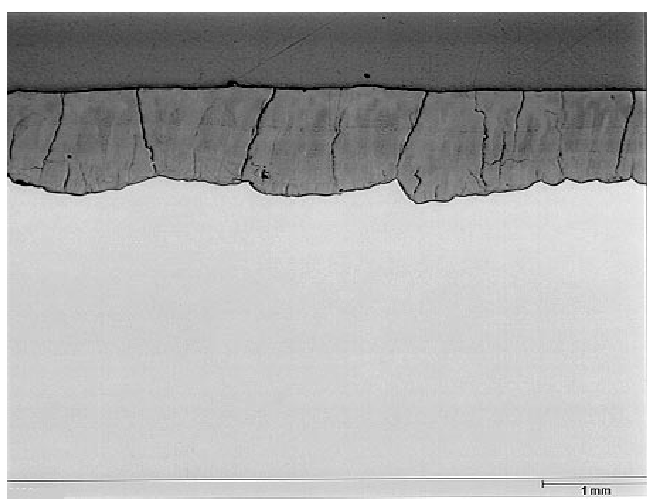

Fig. 3 Al_2O_3/TiO_2 on AlSi10Mg. Cross section of overlapping tracks

chemically most stable and hardest modification of Al_2O_3. The formation of α-Al_2O_3 illustrates an advantage of these coatings over plasma-sprayed coatings because plasma-sprayed coatings always contain a certain amount of metastable γ-Al_2O_3.

Scanning electron micrographs reveal a dendritic solidification structure with differently orientated dendrites. In the interdendritic areas between the Al_2O_3 dendrites, a titanium-rich phase was detected by EDXA (see Fig. 4). This phase might consist of Al_2TiO_5. According to the phase diagram (Ref 13), Al_2TiO_5 only exists at high temperatures. However, because of the relatively high cooling rates, the solidification is a nonequilibrium process and this phase can also be found at room temperature. The titanium-depleted zone at the coating/substrate interface is determined by the solidification kinetics (Fig. 5). Good bonding to the substrate is in large part due to a chemical bond between Al_2O_3 and the aluminum alloy. The bonding defects that still occur are often only a local clustering of small, porelike defects at the interface. Their formation could possibly result from the formation of suboxides or shrinkage effects.

Using pure Al_2O_3 powder, layers with a thickness of 50 to 300 µm could be produced, which, however, partly exhibit bonding defects as well as transcrystalline and intercrystalline cracks. The layer structure can be described as compact and almost free of pores and precipitate. The use of a linear beam profile improved the uniformity of the track geometry, yet it led at first to lower layer thicknesses and problems with track overlapping. Therefore, after grinding, a sufficiently thick and uniform layer could not be guaranteed. However, enough potential for further parameter and beam variations remains that further investigations will be made with Al_2O_3.

Zirconia and mullite additions to Al_2O_3 powder proved to be unsuitable. The produced layers have numerous cracks and bonding defects, as well as a very uneven geometry, especially with overlapping tracks.

Cladding with Y_2O_3-stabilized ZrO_2 led to tracks with a uniform geometry, but the layers show a clear tendency to form horizontal cracks close to the substrate interface. This phenomenon, which has a negative effect on the adhesive strength, is obviously a result of the brittleness and very high melting

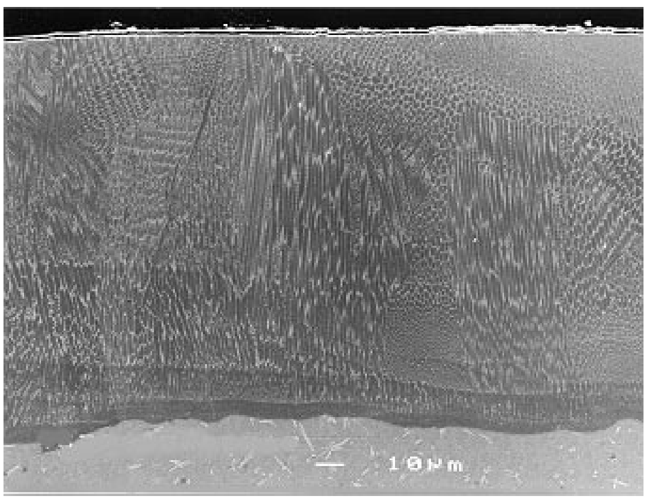

Fig. 4 Typical structure of the Al_2O_3/TiO_2 coatings

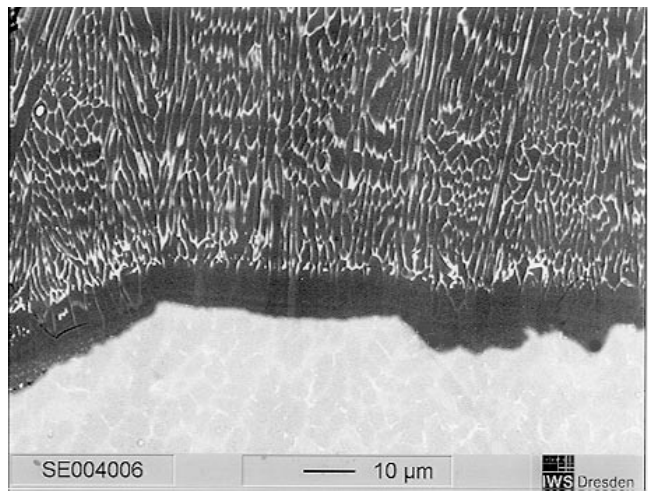

Fig. 5 Titanium-depleted interface zone between ceramic coating and AlSi10Mg-substrate

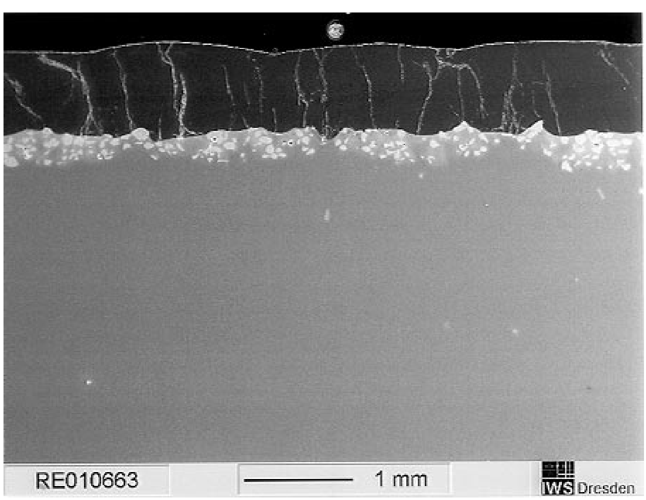

Fig. 6 Al_2O_3/TiO_2 on TiAl6V4. Cross section of overlapping tracks

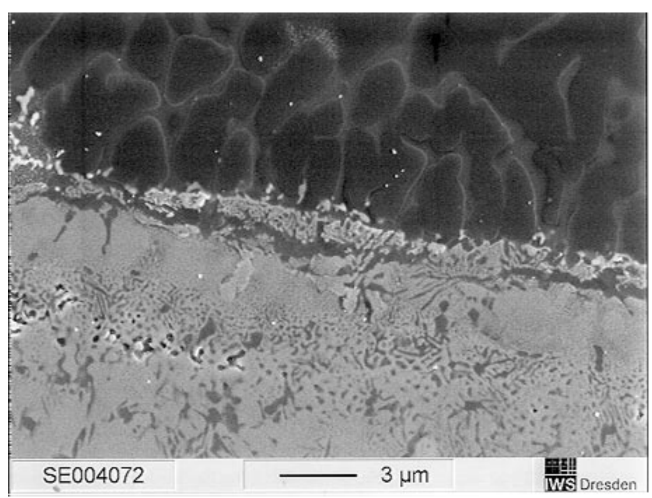

Fig. 7 Diffusion zone between coating and TiAl6V4 substrate

temperature of ZrO_2 and the related and unfavorable residual stress state after solidification. On the other hand, a marked chemical reaction between the layer and the aluminum substrate material takes place, which leads to the formation of several different phases. From this, an improvement of the adhesion is to be expected.

Al_2O_3/TiO_2 (87/13) on TiAl6V4. The ceramic coatings obtained are 0.5 to 1.1 mm thick and well bonded to the base metal. They are dense and show a good uniformity and a homogeneous network of vertical cracks (Fig. 6). Single tracks are less susceptible to crack formation. A high-melting metallic bond coat was used to obtain a high adhesive strength for the bond between the ceramic and the titanium alloy substrate. The bonding mechanisms are mainly based on chemical interactions. The interface between the ceramic and the base metal is marked by a diffusion zone (Fig. 7). Isolated bonding defects, which occur in the form of thin cracks at the interface, are a result of shrinkage effects.

4.2 Hardness

The hardness (average of ten measurements) of the oxide ceramic layers is listed in Table 2. The values of the Al_2O_3-based coatings lie in the typical range for this type of ceramics, between 1800 and 2000 HV0.1. It is noticeable that the layer hardness decreases with increasing TiO_2 content in the powder, as is known to be the case for plasma-sprayed layers (Ref 14). As expected, the hardness value of the ZrO_2/Y_2O_3 coatings approaches that of compact ZrO_2 ceramics (1600 HV0.1).

4.3 Adhesive Strength

The adhesive strength of the ceramic-aluminum bond was investigated with a specially developed adhesion test apparatus (Fig. 8), and the results were compared with those of plasma-sprayed layers of comparable compositions. For each coating material, six tests were used to find the stated averages. As shown in Fig. 9, the results of the laser-coated samples have a clear dependency on the type of ceramic coating. The highest values are achieved with the layers made from Al_2O_3/TiO_2, whereby the layer with the higher TiO_2 content exhibits a better adhesive strength. The corresponding values are nearly 2.5 times higher than values for the plasma-sprayed layers. The fracture behavior was characterized by the fact that the surface of the test specimens was still partly or completely coated with the ceramic after fracture. Since the fracture took place at these points in the coatings, the measured values reflect the fracture strength of the coatings. In contrast, the plasma-sprayed coatings failed almost without exception at the bond zone between the ceramic and the metal.

The reasons for the lower values of the laser-generated ZrO_2 and Al_2O_3 coatings are the partly strong segmentation, the presence of horizontally extending cracks, and the partial formation of pores close to the adhesion region.

Table 2 Powder composition and hardness of the coatings

Coating material	Composition, wt%	Type	Hardness HV0.1
Al_2O_3		…	2000
Al_2O_3/TiO_2	93/7	Mixed powder	2000
Al_2O_3/TiO_2	88/12	Mixed powder	1850
Al_2O_3/TiO_2	87/13	Composite powder	1900
Al_2O_3/TiO_2	55/45	Composite powder plus TiO_2	1400
Al_2O_3/Mullite	75/25	Mixed powder	1900
$Al_2O_3/(ZrO_2\text{-}Y_2O_3)$	84/16	Mixed powder	1900
$ZrO_2\text{-}Y_2O_3$	93/7	Composite powder	1600

5. Finishing

Planar grinding was performed successfully on the Al_2O_3/TiO_2 layers. The surfaces could be levelly ground with a diamond disc without spalling or other undesired accompanying phenomena. Thus, it is expected that there would be no problems with respect to the workability of the coated samples and parts. After grinding, a regular network of fine, process-dependent cracks could be observed on the sample surfaces.

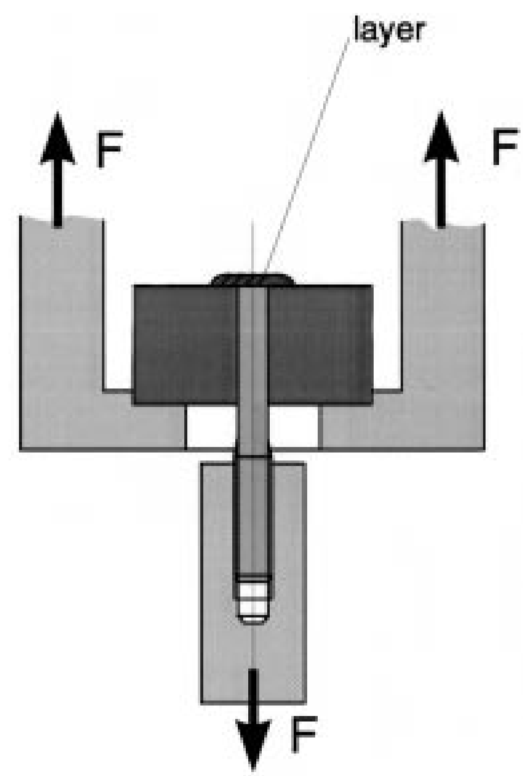

Fig. 8 Sample geometry and principle of the adhesion test

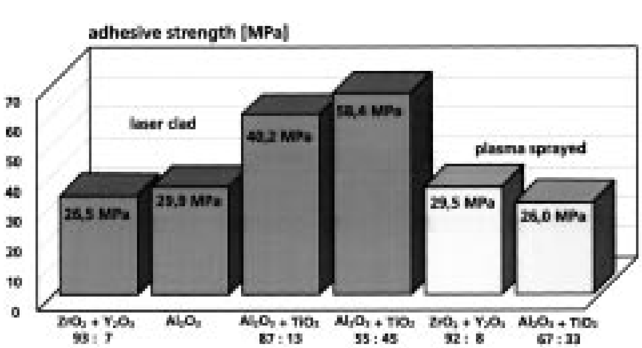

Fig. 9 Results of the adhesion investigation

Peer Reviewed

6. Conclusions

Recently, laser cladding with dynamic powder feed has been successfully applied to produce dense ceramic coatings on commonly used aluminum and titanium alloys. The best results were achieved with an Al_2O_3/TiO_2 composite powder. Layers in this material have a compact and nonporous cast structure and a high adhesive strength with respect to the substrate material. The main component of the coatings was found to be α-Al_2O_3. The interdendritic areas mainly consist of Al_2TiO_5. The thickness of the even and precisely localized coatings is up to 1 mm.

The laser technique is also suitable for the production of dense ZrO_2/Y_2O_3 coatings. However, the presence of horizontal cracks decreases the adhesive strength and makes further investigations to optimize the cladding parameters necessary.

Finish machining can be performed easily by grinding with a diamond disc. This new cladding method is being developed for the surface protection of complex loaded components of automobile and plane engines.

References

1. J. Drozak, Properties of Particles and Adhesion at Thermal Spraying of Metal and Ceramic, *VDI-Fortschrittberichte*, Reihe 5 (No. 361), VDI-Verlag, 1994 (in German)
2. H.-D. Steffens, Z. Babiak, and M. Gramlich, Production of Thick Thermal Barrier Coatings of ZrO_2-Y_2O_3 with Optimized Lifetime, *Proc. of DLR-Workshop "Gradientenwerkstoffe,"* 11.11, Köln, 1993 (in German)
3. R. Agethen and E. Lugscheider, Adhesion Strength of Thermal Sprayed Coatings, *VDI-Bericht No. 702,* VDI-Verlag, 1988, p 197-213 (in German)
4. S.Z. Lee and K.-H. Zum Gahr, Surface Treatments of Al_2O_3-Ceramics by CO_2-Lasers, *Materialwiss. und Werkstofftechn.,* Vol 23, 1992, p 117-123
5. P.C. Tsai, H.L. Tsai, and D.C. Tu, Effect of Processing Parameters on Laser Glazing of Plasma Sprayed YSZ, in *Proc. of LAMP '92,* Nagaoka, June 1992, p 877-882
6. R. Sivakumar and B.L. Mordike, Laser Melting of Plasma Sprayed Ceramic Coatings, *Surf. Eng.,* Vol 4 (No. 2), 1988, p 127-140
7. B. Grünenwald, Beam Combining for Laser Surface Treatment with Additional Material, *Final Report,* Dresden, Stuttgart, March 1995 (in German)
8. S. Nowotny, A. Müller, and A. Techel, Mechanical Properties of Laser Claddings of WC-Reinforced Hard Alloys, *DVS-Berichte,* Vol 175, 1996, p 155-159 (in German)
9. E. Ramous, L. Giordano, and A. Tiziani, Laser Cladding of Ceramic and Metallic Coatings on Steel, *Proc. of Surface Engineering with High Energy Beams,* 2nd International Seminar, Lisboa, 1989
10. E. Lugscheider, H. Bolender, K. Hochmuth, and G. Herziger, One-Step Powder Cladding of Oxide Ceramics onto Metal Substrates with CO_2-Laser Radiation, *DVS-Berichte,*Vol 163, 1994, p 213-218
11. Y.T. Pei, J.H. Ouyang, and T.C. Lei, Laser Cladding of ZrO_2-(Ni-Alloy) Composite Coating, *Surf. Coat. Technol.,* Vol 81, 1996, p 131-135
12. R. Gassmann and M.F. Modest, Laser Cladding of PSZ on Titanium, Nickel, and Steel Alloys, *Proc. of ICALEO 1994,* 17-20.10, 1994, p 125-133
13. S.M. Lang, C.L. Fillmore, and L.H. Maxwell, *J. Nat. Bur. Standards,* Vol 4 (No. 84), 1952, p 301
14. J. Beczkowiak, X. Laufenburg, and H. Keller, Al_2O_3/TiO_2 Coatings: An Alternative to Cr_2O_3?, *DVS-Berichte,* Vol 175, 1996, p 68-71 (in German)